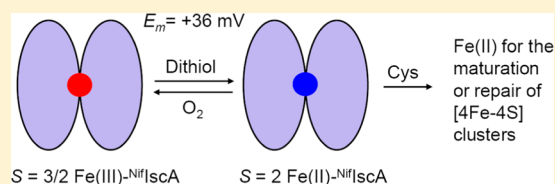


Spectroscopic and Functional Characterization of Iron-Bound Forms of *Azotobacter vinelandii* Nif^IIscADaphne T. Mapolelo,^{§,1} Bo Zhang,[§] Sunil G. Naik,[#] Boi Hanh Huynh,[#] and Michael K. Johnson^{*,§}[§]Department of Chemistry and Center for Metalloenzyme Studies, University of Georgia, Athens, Georgia 30602, United States[#]Department of Physics, Emory University, Atlanta, Georgia 30322, United States

S Supporting Information

ABSTRACT: The ability of *Azotobacter vinelandii* Nif^IIscA to bind Fe has been investigated to assess the role of Fe-bound forms in NIF-specific Fe–S cluster biogenesis. Nif^IIscA is shown to bind one Fe(III) or one Fe(II) per homodimer and the spectroscopic and redox properties of both the Fe(III)- and Fe(II)-bound forms have been characterized using the UV–visible absorption, circular dichroism, and variable-temperature magnetic circular dichroism, electron paramagnetic resonance, Mössbauer and resonance Raman spectroscopies. The results reveal a rhombic intermediate-spin ($S = 3/2$) Fe(III) center ($E/D = 0.33$, $D = 3.5 \pm 1.5 \text{ cm}^{-1}$) that is most likely 5-coordinate with two or three cysteinate ligands and a rhombic high spin ($S = 2$) Fe(II) center ($E/D = 0.28$, $D = 7.6 \text{ cm}^{-1}$) with properties similar to reduced rubredoxins or rubredoxin variants with three cysteinate and one or two oxygenic ligands. Iron-bound Nif^IIscA undergoes reversible redox cycling between the Fe(III)/Fe(II) forms with a midpoint potential of $+36 \pm 15 \text{ mV}$ at pH 7.8 (versus NHE). L-Cysteine is effective in mediating release of free Fe(II) from both the Fe(II)- and Fe(III)-bound forms of Nif^IIscA. Fe(III)-bound Nif^IIscA was also shown to be a competent iron source for in vitro NifS-mediated [2Fe-2S] cluster assembly on the N-terminal domain of NifU, but the reaction occurs via cysteine-mediated release of free Fe(II) rather than direct iron transfer. The proposed roles of A-type proteins in storing Fe under aerobic growth conditions and serving as iron donors for cluster assembly on U-type scaffold proteins or maturation of biological [4Fe-4S] centers are discussed in light of these results.



Iron–sulfur cluster biosynthesis in bacteria involves three distinct types of biosynthetic machinery termed the nitrogen fixation (NIF), iron–sulfur cluster (ISC), and sulfur utilizing factor (SUF) systems.^{1–4} The NIF system (NifS, NifU, and Nif^IIscA) is a specialized system for maturation of the Fe–S proteins involved with nitrogen fixation,⁵ while the ISC system (IscR, IscS, IscU, IscA, HscAB, Fdx, IscX) is responsible for general or housekeeping Fe–S cluster biosynthesis.⁶ In contrast, the SUF system (SufA, SufBCD, SufSE) appears to be a backup system that functions under Fe limitation or oxidative stress conditions in many bacteria, although it is the only system for Fe–S cluster biogenesis in cyanobacteria and in many archaea.⁷ In accord with evolutionary and O₂-tolerance considerations, the ISC and SUF systems form the basis of eukaryotic mitochondrial and plastid Fe–S cluster biogenesis machineries, respectively. The primary components of each of these systems were initially indicated based on the organization of genes in the *nif*, *isc*, and *suf* operons and each appears to involve cysteine desulfurase (NifS, IscS, and SufSE)-mediated Fe–S cluster assembly on a primary scaffold protein (NifU, IscU, and SufB) followed by intact cluster transfer to apo forms of acceptor Fe–S proteins.^{8–16} While the cysteine desulfurase is clearly the S donor, many questions remain concerning the nature of the Fe donor, the mechanism of cluster assembly and transfer to wide variety of acceptor proteins, and the role of the ubiquitous A-type Fe–S cluster biogenesis proteins which are

present in the NIF, ISC, and SUF systems (Nif^IIscA, IscA, and SufA).

The A-type proteins are small proteins, approximately 110 amino acids in bacterial proteins and eukaryotic proteins that lack targeting sequences, with three highly conserved cysteine residues in a C-X_n-C-G-C sequence motif (*n* is usually 63–65, but is increased by a 21-residue insert in some eukaryotic proteins such as *Saccharomyces cerevisiae* Isa2). All three of the conserved cysteine residues are essential for function based on in vivo yeast mutagenesis studies.^{17,18} Crystal structures have been reported for the apo forms of *Escherichia coli* IscA^{19,20} and SufA²¹ and an NMR structure has been reported for *Aquifex aeolicus* IscA.²² The structures all show a novel protein fold, but were of limited utility for addressing the site for Fe or Fe–S cluster binding as the N-terminal C-G-C motif was generally not observed, presumably because of conformational flexibility. Moreover, the *E. coli* IscA structures were homotetramers rather than the homodimeric forms that predominate in solution. Only the *E. coli* SufA crystallized in a dimeric form with the C-G-C motif observable in one subunit in an arrangement that suggested that the two C-G-C motifs would be in close proximity at the subunit interface and hence be available for Fe or Fe–S cluster ligation.²¹ More recently, the

Received: May 21, 2012

Revised: September 7, 2012

Published: September 24, 2012

crystal structure of a [2Fe-2S] cluster-bound form of *Thermosynechococcus elongatus* IscA revealed an asymmetric tetramer involving similar α subunits and domain-swapped β subunits with two subunit bridging [2Fe-2S] clusters.²³ The domain swapping has been attributed to a crystallization artifact and molecular modeling studies suggest that the asymmetric cluster ligation, involving the three conserved cysteines from the α subunit and the N-terminal conserved cysteine of the β subunit, is most likely retained in a functional asymmetric $\alpha\beta$ dimer. Such asymmetric cluster ligation provides an attractive mechanism for cluster assembly/incorporation and release.²³

A variety of different functions have been proposed for A-type proteins in Fe–S cluster biogenesis based on a combination of in vivo and in vitro evidence. These include roles as alternative scaffold proteins for de novo cluster biosynthesis,^{24,25} carrier proteins for delivery of clusters preassembled on scaffold proteins,^{16,26,27} regulatory proteins for iron homeostasis and the sensing of redox stress,²⁸ and specific Fe-donors for cluster assembly on U-type scaffold proteins²⁹ or maturation of mitochondrial [4Fe-4S] centers.³⁰ In large part, the lack of a current consensus concerning function stems from the fact that the effects of single gene knockouts in bacteria are generally minor except for growth under elevated levels of O₂³¹ and that multiple A-type proteins exhibiting considerable functional redundancy are present in many organisms.^{27,32} However, recent in vivo studies involving functional characterization of multiple gene deletions of bacterial A-type proteins have revealed strong phenotypes. For example, *E. coli* *iscA* and *sufA* double mutants have demonstrated an essential role for A-type proteins in the maturation of [4Fe-4S] centers under aerobic growth conditions.^{27,32,33} Moreover, individual gene knockouts of *S. cerevisiae* *Isa1* and *Isa2* and human *ISCA1* and *ISCA2* displayed severe phenotypes that are associated with ineffective maturation of mitochondrial [4Fe-4S] cluster-containing enzymes.^{30,34}

The work presented herein was designed to assess the proposal that A-type proteins function as specific Fe donors for Fe–S cluster assembly on U-type scaffold proteins by investigating the ability of Nif⁺IscA to bind Fe and to assess if Fe-bound forms can function as specific Fe donors for Fe–S cluster assembly of on NifU. In vitro studies of *E. coli* *IscA* and *SufA* and human *ISCA1*, Ding and co-workers have shown that A-type Fe–S cluster biogenesis proteins are competent Fe donors for cluster assembly on the U-type class of primary scaffold proteins.^{29,32,35–41} The conserved C-terminal CGC cysteines of A-type proteins have been shown to be essential for high affinity binding of Fe(III) which can be specifically mobilized by L-cysteine for in vitro assembly on IscU.^{29,32,35–37} Further support for an Fe donor role comes from the ability of A-type proteins to recruit iron for Fe–S cluster biosynthesis in vitro from the iron-storage protein ferritin in the presence of the thioredoxin reductase system³⁸ or under conditions of limited accessible free-iron³⁷ and to store Fe(III) in an accessible form for cluster assembly under aerobic growth conditions.^{32,42}

However, spectroscopic characterization of Fe-bound forms of A-type proteins have been limited to UV–visible absorption and EPR and, notably, Mössbauer studies have failed to confirm high affinity iron binding to the conserved cysteine residues of *E. coli* *SufA*.⁴³ In addition, the lack of an observable phenotype for double *iscA* and *sufA* mutant strains under anaerobic conditions,^{27,32} coupled with the in vivo evidence that Fe–S

cluster formation on Isu1 and Isu2 in yeast mitochondria does not require *Isa1* or *Isa2*,³⁰ indicate that A-type proteins cannot be the sole Fe donors for cluster assembly on U-type proteins.

The recent comprehensive in vivo studies of the role of *Isa1/Isa2* in yeast Fe–S cluster biogenesis have raised the possibility of an alternative, albeit ill-defined, role for Fe-bound A-type proteins.³⁰ This work provides compelling evidence that an Fe-bound form of the *S. cerevisiae* *Isa1-Isa2* complex is present in vivo and is specifically required, along with *Iba57* (which releases the Fe) and *Isu1/Isu2*, for the general maturation of mitochondrial [4Fe-4S] cluster-containing proteins, rather than functioning as a specific Fe donor for cluster assembly on the *Isu1/Isu2* scaffold proteins.³⁰

In principal, the simplicity of the NIF system for Fe–S cluster biogenesis, which comprises only NifS (S-donor), NifU (scaffold for cluster assembly), and Nif⁺IscA, and is limited to the maturation of single and double cubane [4Fe-4S] centers in nitrogen fixation proteins, makes Nif⁺IscA an excellent candidate for elucidating the function of A-type proteins. Hence, the objectives of this study were to prepare and investigate the detailed electronic, magnetic, redox, and vibrational properties of iron-bound forms of *Azotobacter vinelandii* (Av) Nif⁺IscA, as a precursor to understanding the role of Nif⁺IscA in Nif-specific Fe–S cluster biogenesis. Thus far spectroscopic characterization of Fe-bound forms of A-type Fe–S cluster biogenesis proteins have been limited to UV–visible absorption and EPR studies of ferric-bound *E. coli* *IscA* and *SufA* and human *ISCA1*.^{29,32,35} In this work, the spectroscopic and redox properties of both the Fe(III)- and Fe(II)-bound forms of Av Nif⁺IscA have been investigated by the combination of UV–visible absorption, circular dichroism (CD) and variable-temperature magnetic circular dichroism (VTMCD), electron paramagnetic resonance (EPR), resonance Raman and Mössbauer spectroscopies. The results provide insight into the ground and excited state properties and ligation of both the Fe(III)- and Fe(II)-bound forms, demonstrate that the Fe in both forms is released by L-cysteine, and facilitate determination of the one-electron redox potential for Fe(III)/Fe(II)-bound Nif⁺IscA. In addition, Fe(III)-bound Nif⁺IscA is shown to be an effective but nonspecific Fe donor for [2Fe-2S] cluster assembly on N-terminal IscU-like domain of NifU. Overall, the results support the view that A-type proteins provide a means of storing Fe(III) under aerobic growth conditions in an accessible form for use in Fe–S cluster biogenesis and possible roles are discussed.

MATERIALS AND METHODS

Materials. Materials used in this work were of reagent grade and were purchased from Fischer Scientific, Sigma-Aldrich Chemical Co, Invitrogen, or VWR International, unless otherwise stated.

Expression and Purification of Av Nif⁺IscA and NifU-1. The *A. vinelandii* Nif⁺*iscA* gene, encoding the Nif⁺IscA protein, was amplified by PCR and inserted into the expression plasmid PT-7 as previously described.²⁴ The resulting plasmid, pDB570, was transformed into the *E. coli* host BL21 (DE3) and induced for high level expression of Av Nif⁺IscA according to the published procedure.²⁴ Av Nif⁺IscA was purified under aerobic conditions by suspending cell paste (60.0 g) in 120 mL of 50 mM Tris-HCl buffer pH 7.8 (buffer A) containing 2 mM β -mercaptoethanol and disrupting the cells by sonication on ice for 45 min. After centrifugation at 17 000 rpm for 1 h at 4 °C, the crude extract was treated with 1% (w/v) streptomycin

sulfate and incubated at room temperature for 5 min before recentrifugation. The supernatant was then precipitated with 40% ammonium sulfate and the pellet was resuspended in buffer A and then loaded on a Q-Sepharose (Pharmacia) column (50 mm inner diameter, 110 mL) equilibrated with buffer A. Elution was achieved with a 0.0–1.0 M NaCl gradient in buffer A, with Nif^{IscA} eluting between 0.49 and 0.53 M NaCl and pooled as single fraction. This fraction was then concentrated down to 3 mL using Amicon ultrafiltration with a YM10 membrane and loaded on a 200 mL Superdex S75 gel-filtration column previously equilibrated with 100 mM Tris-HCl buffer pH 7.8, with 150 mM NaCl. On the basis of gel electrophoresis analysis, the last fraction to elute from the Superdex-75 column was concentrated as above and frozen as pellets in liquid nitrogen until used. The purity of this fraction was estimated to be approximately 95% based on gel electrophoresis. The yield of Nif^{IscA} from 60 g of cells was approximately 50 mg. Expression and purification of *A. vinelandii* NifU-1, a truncated form of NifU containing only the N-terminal U-type domain, was carried out as previously described.^{44,45}

Chemical Analyses. Nif^{IscA} protein concentrations were determined using bovine serum albumin as a standard (Roche) with BioRad Dc protein assay in conjunction with the microscale modified procedure of Brown et al.⁴⁶ The purity and concentration of Nif^{IscA} samples were also assessed by direct amino acid analyses conducted at Texas A&M University using samples dialyzed against water in a YM10 centricon to remove Tris base which interferes with the assay. On the basis of parallel direct amino acid analyses and BioRad Dc protein assays on identical samples, the BioRad Dc protein assay was found to over estimate the protein concentration of Nif^{IscA} by 17%. All Nif^{IscA} concentrations are based on protein monomer unless otherwise stated. Iron concentrations were determined after KMnO_4/HCl protein digestion as described by Fish,⁴⁷ using a 1000 ppm atomic absorption iron standard to prepare standard solutions of known Fe concentration (Fluka). Metal analyses of as purified Nif^{IscA} samples were carried in the ICP-MS facility in Dr. Michael Adams laboratory at the University of Georgia.

Preparation of Fe-Bound Nif^{IscA} . All sample preparation procedures were carried out under strictly anaerobic conditions inside a Vacuum Atmospheres glove under argon (<2 ppm O_2), unless otherwise noted. Ferric-bound Nif^{IscA} was prepared by treating Nif^{IscA} (0.8 mM) in 100 mM Tris-HCl buffer, pH 7.8, with 150 mM NaCl with 800 mM Tris(hydroxypropyl)phosphine (THP) to cleave disulfides followed by titration with ferric ammonium citrate at room temperature. The Fe-loaded Nif^{IscA} was then passed through a 50 mL desalting column to remove any adventitiously bound iron. The fraction which contained the Fe-bound Nif^{IscA} was concentrated by Amicon ultrafiltration using a YM10 membrane. Ferrous-bound Nif^{IscA} was prepared by reducing purified ferric-bound Nif^{IscA} with a 5-fold excess of sodium dithionite under anaerobic conditions. Both the ferric-bound and ferrous-bound Nif^{IscA} were analyzed for Fe and protein before being spectroscopically characterized.

EPR-Monitored Redox Titrations. EPR redox titrations were performed at ambient temperature (25–27 °C) inside the glovebox under anaerobic conditions using 0.4 mM Fe-bound Nif^{IscA} in a 50 mM Tris-HCl buffer, pH 7.8. THP was completely removed by repeated dialysis prior to conducting redox titrations. Mediator dyes were added, each to a concentration of ca. 50 μM , in order to cover the desired

range of redox potentials, i.e., 1,4-benzioquinone (+274 mV), 1,2-naphtho-4-sulfonate (+215 mV), 1,2-naphthoquinone (+134 mV), 1,4-naphthoquinone (+69 mV), methylene blue (+11 mV), indigo-disulphonate (–125 mV), anthraquinone-1,5-disulphonate (–170 mV), phenosafranin (–252 mV), safranin O (–289 mV), and neutral red (–325 mV). Samples were first oxidized with a minimal excess of potassium ferricyanide followed by reductive titration with sodium dithionite and reoxidation to the starting potential with ferricyanide to check for reversibility. After equilibration at the desired potential, a 0.25-mL aliquot was transferred to a calibrated EPR tube and immediately frozen in liquid nitrogen. Potentials were measured using a platinum working electrode and a saturated Ag/AgCl reference electrode. All redox potentials are reported relative to the normal hydrogen electrode (NHE). The EPR signal intensities from samples collected at different potentials were fitted to a one-electron Nernst equation.

Determination of the Oligomeric State of Apo and Fe-Bound Nif^{IscA} . The oligomeric state of apo and Fe-bound forms of Nif^{IscA} were assessed by gel-filtration chromatography using a 25 mL Superdex G-75 10/300 column (Pharmacia Biotech), equilibrated with 50 mM Tris-HCl buffer with 100 mM KCl (pH 7.6) and using a flow rate of 0.4 mL/min. The molecular weight standards used were aprotinin (M_r 6500), albumin (M_r 66 000), blue dextran (M_r 2 000 000), carbonic anhydrase (M_r 29 000), and cytochrome *c* (M_r 12 400) (Sigma-Aldrich).

Spectroscopic Methods. All samples for spectroscopic investigations were prepared under an argon atmosphere in the glovebox unless otherwise noted. UV–visible absorption and CD spectra were recorded in sealed anaerobic 1 mm quartz cuvettes at room temperature, using a Shimadzu UV-3101 PC scanning spectrophotometer and a Jasco J-715 spectropolarimeter, respectively. Resonance Raman spectra were recorded at 17 K on frozen droplets of sample mounted on the coldfinger of a Displex model CSA-202E closed cycle refrigerator (Air Products, Allentown, PA) as previously described,⁴⁸ using a Ramanor U1000 scanning spectrometer (Instruments SA, Edison, NJ) coupled with a Sabre argon-ion laser (Coherent, Santa Clara, CA). VTMCD spectra were recorded on anaerobically prepared samples containing 55% (v/v) ethylene glycol to enable the formation of good optical-quality glasses upon rapid freezing. Spectra were recorded with Jasco J-715 spectropolarimeter (Jasco, Easton, MD) mated to an Oxford Instruments Spectromag 4000 cryostat/magnet capable of generating magnetic fields of up to 7 T and maintaining sample temperatures in the range 1.5–300 K, using the protocols described elsewhere.^{49,50} VHTV MCD saturation magnetization data at discrete wavelengths were collected by increasing the field from 0 to 6 T at fixed temperatures of 1.73, 4.22, 10.0, and 25.0 K and analyzed according to the published procedures using software supplied by Edward I Solomon (Stanford University).⁵¹ X-band (~9.6 GHz) EPR spectra were recorded using a ESP-300D spectrometer (Bruker, Billerica, MA) equipped with an ER-4116 dual mode cavity and an ESR 900 flow cryostat (Oxford Instruments, Concord, MA). Mössbauer spectra of ^{57}Fe -enriched samples in the presence of weak and strong applied magnetic fields were recorded using the instrumentation previously described,⁵² and analyzed using WMOSS software (Web Research).

RESULTS

Fe Binding to *A. vinelandii* $NifIscA$. In previous studies of iron-binding by $Av^{NifIscA}$, there was no evidence for bound iron in as-purified recombinant samples based on ICP-AES and no evidence for ferric binding in titration experiments monitored by UV–visible absorption, VTMCD and Mössbauer spectroscopies.²⁴ Substoichiometric ferrous binding in a rubredoxin-type environment was observed in samples treated with a 4–10 fold excess of Fe(II) based on UV–visible absorption, VTMCD and Mössbauer studies. However, the bound iron was lost during gel filtration to remove excess iron, indicating low binding affinity. These experiments were all conducted under strictly anaerobic conditions in samples that were pretreated with DTT to cleave disulfides and then repurified under anaerobic conditions to remove DTT. This was necessary because DTT forms a complex with both ferric and ferrous ions in aqueous solution as evident by UV–visible absorption, VTMCD and Mössbauer spectroscopies. Hence, our initial reaction to the reports by Ding et al.²⁹ of ferric binding to *E. coli* *IscA* on aerobic addition of Fe(II) in the presence of DTT was that the Fe(III)-bound *IscA* complex may involve exogenous DTT. This possibility was subsequently discounted based on the ability to form the same species in *E. coli* *IscA* using the thioredoxin reductase system in place of DTT.³⁹ Nevertheless we were still unable to induce high affinity ferric or ferrous binding to $Av^{NifIscA}$ even in the presence of DTT under aerobic or anaerobic conditions.

The origin of the inability of $Av^{NifIscA}$ to bind iron in a high affinity ferric site was suggested by the observation that the protein is purified in the apo form essentially devoid of bound Fe (<0.02 Fe/monomer), as judged by ICP-MS analysis, even though samples invariably exhibit a 320 nm band that has been attributed to the Fe(III)-bound forms of *E. coli* *IscA* and *SufA*.^{29,32} Furthermore, addition of EDTA or DTT did not decrease the intensity of the 320-nm band. However, the addition of tris(hydroxypropyl)phosphine (THP), an alternative, non-thiol-based disulfide/polysulfide cleaving reagent, resulted in substantial loss of the 320-nm band suggesting that it originates from polysulfides that are not accessible or reducible by DTT. Moreover, $Av^{NifIscA}$ was found to bind Fe(III) in the presence of THP under both aerobic and anaerobic conditions. This is illustrated in Figure 1 which shows a titration of $Av^{NifIscA}$ with ferric ammonium citrate under aerobic conditions in the presence of 100 mM THP. The results demonstrate tight binding of Fe(III) with a stoichiometry of 0.5 Fe/ $NifIscA$ monomer which corresponds to 1.0 Fe/ $NifIscA$ dimer, since the apo protein and the Fe(III)-bound form were both determined to be dimers in aqueous solution based on quantitative gel filtration studies (data not shown). The absorption and CD properties of Fe(III)-bound $NifIscA$ were also unchanged after exchange into the equivalent aerobic buffer solution containing 2 mM DTT. On the basis of absorption and CD intensity, partially oxidized samples were obtained for analogous Fe(III) titrations of $NifIscA$ carried out under strictly anaerobic conditions in the presence of THP, indicating partial reduction in the absence of O_2 . The UV–visible absorption characteristics and the Fe(III) binding stoichiometry are in good agreement with the results of Ding et al. for Fe(II) addition to *E. coli* *IscA* under aerobic conditions in the presence of DTT or thioredoxin/thioredoxin reductase.^{29,39} However, in contrast to recombinant *E. coli* *IscA*, the Fe-bound form of recombinant $Av^{NifIscA}$ was not observed for

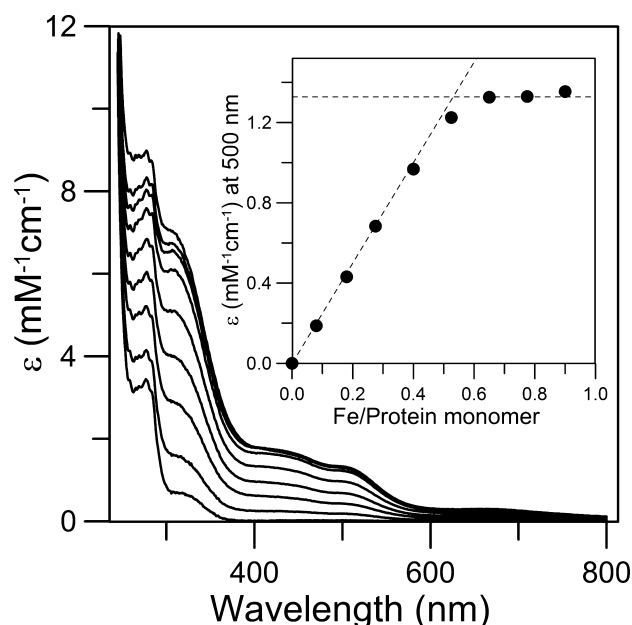


Figure 1. Fe(III) binding to $NifIscA$ monitored by UV–visible absorption spectroscopy. $Av^{NifIscA}$ (0.8 mM) was titrated with ferric ammonium citrate under aerobic conditions in 100 mM Tris/HCl buffer, pH 7.8, in the presence of 100 mM THP. The inset shows a plot of the extinction coefficient at 500 nm as a function of the Fe(III)/ $NifIscA$ monomer ratio. All ϵ values are based on the concentration of $NifIscA$ monomer.

samples isolated from aerobically grown cells and purified under aerobic or strictly anaerobic conditions. Moreover, UV–visible absorption and CD studies of a reconstituted form of $Av^{NifIscA}$ containing one $[2Fe-2S]^{2+}$ cluster per dimer revealed that the Fe(III)-bound form is not a product of O_2 -induced $[2Fe-2S]$ cluster degradation during purification; see Figure S1 in Supporting Information. The results show a gradual loss of the cluster on exposure to air over a 12-h time period, without any evidence for the concomitant appearance of the characteristic absorption or CD spectrum associated with Fe(III)-bound $NifIscA$. Some Fe(III)-bound $NifIscA$ is however formed during the O_2 -induced $[4Fe-4S]$ to $[2Fe-2S]$ cluster conversion on $NifIscA$; see accompanying manuscript in this issue (DOI 10.1021/bi3006658).

Spectroscopic Characterization of Fe-bound *A. vinelandii* $NifIscA$. The Fe(III)-bound form of $NifIscA$ formed by titration with ferric ammonium citrate in the presence of THP can be purified aerobically without loss of Fe and reduced stoichiometrically with sodium dithionite under anaerobic conditions without loss of Fe based on Fe determinations. Moreover, samples can be repeatedly reduced by dithionite and reoxidized by air without significant loss of Fe based on near-quantitative restoration of the visible absorption spectrum on aerial oxidation, see Figure S2 in Supporting Information. The electronic, vibrational and redox properties of the Fe(III)- and Fe(II)-bound forms were therefore investigated using the combination of UV–visible absorption and VTMCD, EPR, Mössbauer, and resonance Raman spectroscopies.

Electronic Excited State Properties. The electronic excited state properties of Fe(III)- and Fe(II)-bound $NifIscA$ were investigated using UV–visible absorption and VTMCD spectroscopies; see Figure 2, panels A and B, respectively. The absorption spectrum of Fe(III)-bound $NifIscA$ comprises

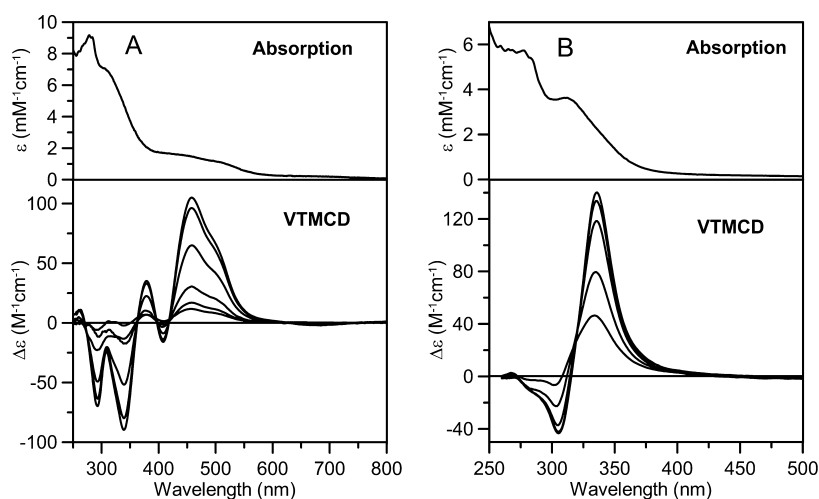


Figure 2. UV–visible absorption and VTMCD spectra for Fe(III)- and Fe(II)-bound NifIscA . All ϵ and $\Delta\epsilon$ values are based on the concentration of NifIscA monomer. (A) Room-temperature absorption and VTMCD spectra of repurified Fe(III)-bound NifIscA (0.9 mM in NifIscA monomer) in 100 mM Tris/HCl buffer, pH 7.8, with 55% v/v ethylene glycol. MCD spectra were recorded for samples in 1 mm cuvettes with a magnetic field of 6 T and at temperatures of 1.73, 4.22, 10, 25, 50, and 100 K. (B) Room-temperature absorption and VTMCD spectra of Fe(II)-bound NifIscA (0.8 mM in NifIscA monomer and reduced under strictly anaerobic conditions with stoichiometric sodium dithionite) in 100 mM Tris/HCl buffer, pH 7.8, 55% v/v ethylene glycol. MCD spectra were recorded for samples in 1 mm cuvettes with a magnetic field of 6 T and at temperatures of 1.73, 4.22, 10, 25, and 60 K. All MCD bands for Fe(III)- and Fe(II)-bound NifIscA increase in intensity with decreasing temperature.

broad CysS-to-Fe(III) charge transfer bands centered near 320, 440, and 520 nm. VTMCD spectra show that the broad and ill-defined absorption spectrum in the CysS-to-Fe(III) charge transfer region results from at least six overlapping C-terms, exhibiting $++--$ signs with increasing energy. Without structural information concerning the Fe(III) coordination environment, it is not possible to make detailed assignments. However, based on the observation that somewhat similar absorption and VTMCD spectra have been observed for single Cys-to-Ser or Cys-to-Asp variants of oxidized rubredoxin⁵³ and a trigonal bipyramidal Fe(III) complex with two equatorial thiolate and three nitrogen ligands,⁵⁴ the data are most consistent with two or three cysteine ligands.

The visible absorption is bleached on reduction and the absorption spectrum of the Fe(II)-bound NifIscA comprises a band centered at 315 nm, with a low-energy shoulder centered near 340 nm. These absorption bands correlate with temperature-dependent MCD bands: positive band centered at 335 nm and negative band centered at 305 nm with a shoulder at ~ 280 nm (Figure 1B). Both the absorption and VTMCD spectra are very similar to those observed for reduced rubredoxin and metallothionein with <4 equiv of Fe(II) bound,⁵⁵ which are attributed to charge transfer transitions associated with a tetrahedrally coordinated high-spin ($S = 2$) Fe(II) center with complete cysteinate ligation. However, the VTMCD $\Delta\epsilon$ values are 2 orders of magnitude lower than those of reduced rubredoxins with all-cysteinate-ligated high-spin Fe(II) centers in a distorted tetrahedral coordination geometry. In contrast, analogous absorption and VTMCD spectra with $\Delta\epsilon$ values similar to observed for Fe(II)-bound NifIscA are exhibited by Cys-to-Asp variants of reduced rubredoxin, which have 4- or 5-coordinate Fe(II) sites involving three cysteinate and a monodentate or bidentate aspartate ligand.⁵³ Hence the absorption and VTMCD data for the Fe(II)-bound NifIscA are most consistent with a 4- or 5-coordinate paramagnetic ferrous site with one or two non-cysteinate ligands.

Electronic Ground State Properties. The ground state electronic and magnetic properties of the Fe(III) and Fe(II)-

bound forms of NifIscA were investigated by EPR and Mössbauer spectroscopies, and VTVH MCD saturation magnetization studies. The X-band EPR spectrum of Fe(III)-bound NifIscA comprises a broad low-field absorption-shaped component with a maximum at $g = 5.5$ and a broad derivative-shaped component centered at $g = 2.0$; see Figure 3A. On the

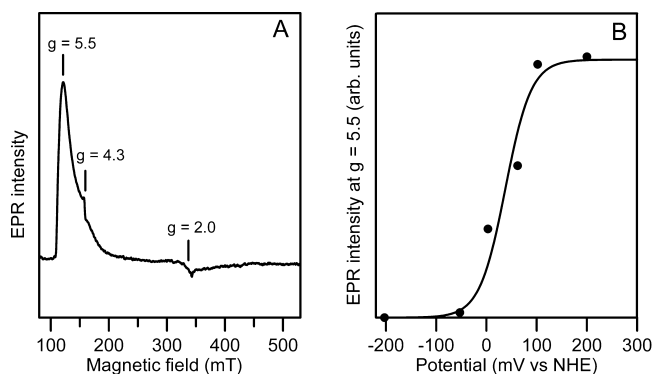


Figure 3. X-band EPR spectrum of Fe(III)-bound NifIscA and EPR-monitored redox titration. Sample is the same as that described in Figure 2A. (A) EPR spectrum recorded at 4.9 K at a microwave frequency of 9.60 GHz, with a modulation amplitude = 0.65 mT and a microwave power of 20 mW. (B) Dye-mediated redox titration of Fe-bound NifIscA monitored by EPR. Solid line is a best fit to a one-electron Nernst plot with a midpoint potential of +36 mV versus NHE.

basis of a conventional $S = 3/2$ spin Hamiltonian, the spectrum is consistent with a rhombic ($E/D = 0.33$) $S = 3/2$ ground state with an isotropic real g -value of 2.0, which predicts effective g values of 5.46, 2.00, and 1.46 for both of the two quantum mechanically mixed Kramers doublets of the $S = 3/2$ manifold. The breadth of the spectrum and the inability to clearly observe the high-field negative absorption-shaped component at $g = 1.46$ is attributed to g -strain originating from heterogeneity in Fe(III) coordination environment. Hence the EPR data

indicates a novel intermediate spin, $S = 3/2$, rhombic Fe(III) center in Fe(III)-bound Nif^{IscA} . This result is in agreement with EPR studies of the Fe-bound forms of *E. coli* IscA and SufA and human ISCA1 which reported weak and ill-defined resonances in the $g = 4$ – 5 region that were interpreted in terms of an $S = 3/2$ Fe(III) center.^{29,32,35}

Additional evidence for a rhombic $S = 3/2$ ground state for Fe(III)-bound Nif^{IscA} came from Mössbauer and VTVH MCD saturation magnetization studies. The Mössbauer spectrum of a partially reduced sample, prepared by adding excess Fe(III) under anaerobic conditions in the presence of THP and repurifying under anaerobic conditions, is shown in Figure 4 (top panel). The spectrum was recorded at 4.2 K with a weak magnetic field of 50 mT applied parallel to γ -beam. It shows a mixture of the oxidized and reduced forms with 45% of the absorption associated with a quadrupole doublet (green line) from the rubredoxin-type high-spin ($S = 2$) Fe(II) species that is present in dithionite-reduced Fe(II)-bound Nif^{IscA} (see below and Figure 5) and the remainder exhibiting magnetic hyperfine structures indicative of a Fe(III) species. To better characterize the Fe(III) species, we also recorded spectra at 4.2 K in 50 mT perpendicular field and in 4 and 8 T parallel fields (data not shown). We then removed the contribution of the rubredoxin-type high-spin Fe(II) species from the raw data by using theoretical simulations (solid lines in Figure 5) of the Fe(II)-bound Nif^{IscA} spectra (Figure 5) recorded at the same applied magnetic fields. The resulting spectra (Figure 4, bottom panel) represent the 4.2 K Mössbauer spectra of the Fe(III) species in 50 mT parallel (A) and perpendicular (C) applied magnetic fields, and in 4 T (C) and 8 T (D) parallel applied fields. The fact that the parallel and perpendicular 50 mT spectra are different indicates nonuniaxial ground state doublets, as expected from the EPR study. Further, in agreement with the EPR results, all four spectra are fit to a good approximation by spin Hamiltonian parameters (listed in Table 1) for a rhombic $S = 3/2$ ground state with $E/D = 0.33$. The values of the zero field splitting parameter, D , and the magnetic hyperfine interaction component, A_{zz} , are highly correlated. It is therefore difficult to get a precise value for one without knowing the other. Nevertheless it is not possible to fit the spectra with $D < 2 \text{ cm}^{-1}$.

Using the Mössbauer and EPR-determined ground-state spin Hamiltonian parameters, VTVH MCD saturation magnetization data for Fe(III)-bound Nif^{IscA} collected at discrete wavelengths can be fit to a good approximation by varying the transition polarizations. This is illustrated for the intense positive MCD band at 458 nm in Figure 6A which shows that the 0–6 T magnetization data collected at 1.73, 4.22, 10.0, and 25 K are well fit by a predominantly xz -polarized transition with effective xy , xz , and yz transition dipole moments, M_{xy} , M_{xz} , M_{yz} , in the ratio 0.2:1.0:0.2. As for the Mössbauer data, the VTVH MCD saturation magnetization data are not very sensitive to the values of D with satisfactory fits possible with D between 1 and 5 cm^{-1} . Taken together, the Mössbauer and VTVH MCD saturation magnetization data confirm a rhombic intermediate spin $S = 3/2$ Fe(III) center in Nif^{IscA} with $E/D = 0.33$ and D between 2 and 5 cm^{-1} .

The dithionite-reduced Fe(II)-bound Nif^{IscA} did not exhibit an X-band EPR signal in parallel or perpendicular mode, but the ground state properties of the paramagnetic ferrous center can be assessed by high-field Mössbauer measurements, see Figure 5, and VTVH MCD saturation magnetization data; see Figure 6B. The 4.2 K Mössbauer spectra recorded with 50 mT,

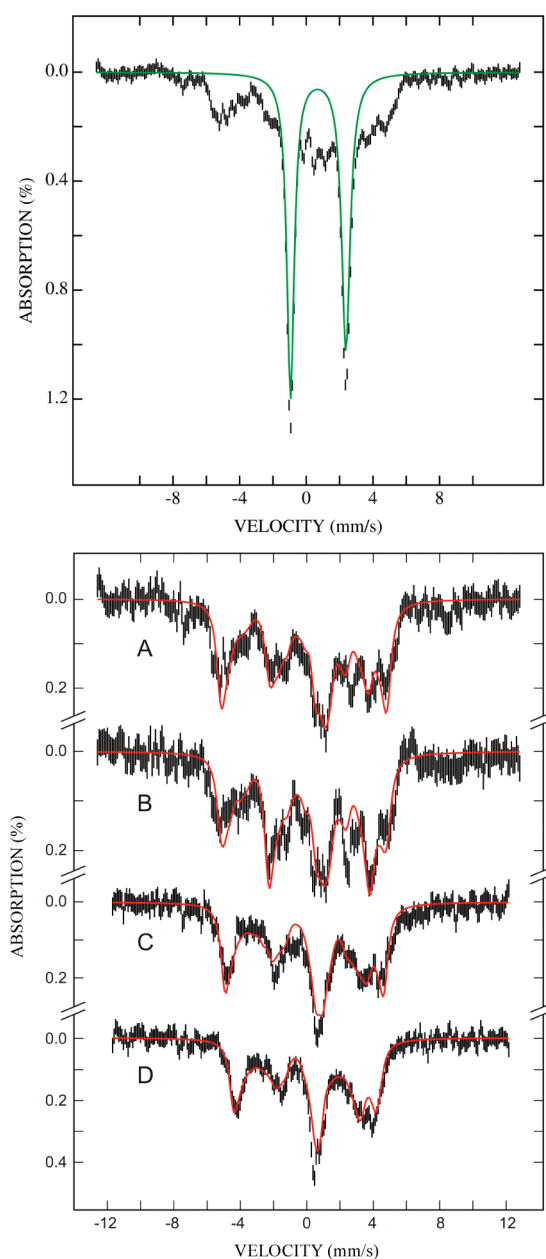


Figure 4. Mössbauer spectra of ^{57}Fe -bound forms of Nif^{IscA} . Top panel: Mössbauer spectrum of a partially reduced ^{57}Fe -bound Nif^{IscA} sample containing both Fe(III)- and Fe(II)-bound forms of the enzyme. The spectrum was recorded at 4.2 K with a field of 50 mT applied parallel to the γ -beam. The solid green line is a quadrupole doublet ($|\Delta E_Q| = 3.33 \text{ mm/s}$ and $\delta = 0.72 \text{ mm/s}$) representing the rubredoxin-type Fe(II)-bound Nif^{IscA} and accounts for 45% of total absorption. Bottom panel: Prepared Mössbauer spectra of Fe(III)-bound Nif^{IscA} after removal of the contribution of the Fe(II)-bound Nif^{IscA} from the raw data (see text). The spectra were recorded at 4.2 K with a field of 50 mT applied parallel (A), 50 mT applied perpendicular (B), 4 T applied parallel (C), and 8 T applied parallel (D) to the γ -beam. Red lines are simulations using parameters (listed in Table 1) that are consistent with an intermediate spin $S = 3/2$ Fe(III) species.

4 and 8 T magnetic fields applied parallel to the γ -ray beam are very similar to those observed for reduced rubredoxins which have rhombic high-spin ($S = 2$) Fe(II) centers with large zero-field splitting in accord with highly distorted tetrahedral ligation by four cysteinate ligand.^{56,57} In fact, the Mössbauer spectra at

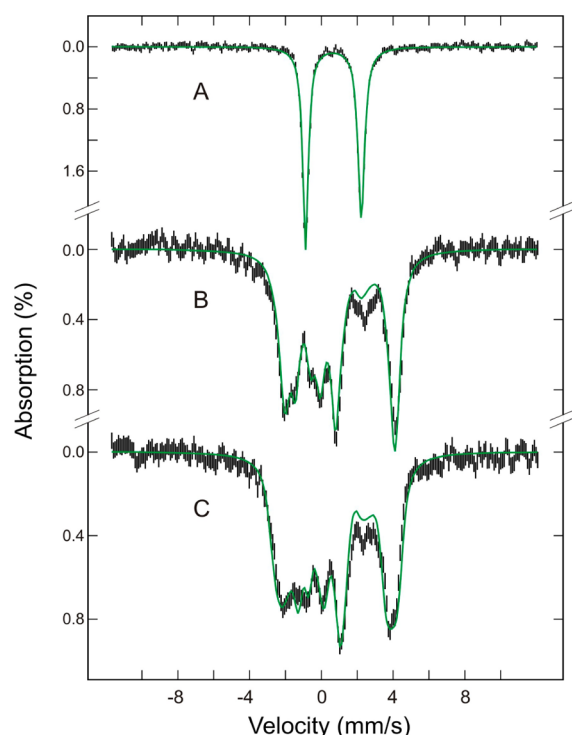


Figure 5. Mössbauer spectra of $^{57}\text{Fe(II)}$ -bound NifIscA . Sample was prepared by dithionite reduction of the sample used in Figure 4. Spectra were recorded at 4.2 K with a magnetic field of 50 mT (A), 4 T (B), and 8 T (C) applied parallel to the γ -beam. The solid green lines overlaid on the experimental spectra are theoretical simulations of a rubredoxin-type Fe(II) species using the parameters listed in Table 1.

Table 1. Spin Hamiltonian Parameters for the Fe(III) -Bound and Fe(II) -Bound Forms of *A. vinelandii* NifIscA as Assessed by Mössbauer Spectroscopy

	Fe(III) -bound NifIscA	Fe(II) -bound NifIscA	<i>C. pasteurianum</i> Fe(II) rubredoxin ^a
S	3/2	2	2
D (cm^{-1})	2–5	7.6 ^a	7.6
E/D	0.33	0.28 ^a	0.28
g_{xx}	2	2.11 ^a	2.11
g_{yy}	2	2.19 ^a	2.19
g_{zz}	2	2.00 ^a	2.00
$A_{xx}/g_n\beta_n$ (T)	–11	–17.5	–20.1
$A_{yy}/g_n\beta_n$ (T)	–21	–7.5	–8.3
$A_{zz}/g_n\beta_n$ (T)	–1	–30.1	–30.1
δ (mm/s)	0.31	0.72	0.7
ΔE_Q (mm/s)	2.83	–3.33	–3.25
η	–0.2	0.85	0.65

^aTaken from ref 56.

all three applied fields can be fit to a good approximation by assuming a rhombic $S = 2$ electronic ground state that is identical to that of reduced *C. pasteurianum* rubredoxin⁵⁶ with slightly modified parameters for the quadrupole and magnetic hyperfine interactions; see Table 1. Likewise the VTVH MCD saturation magnetization data collected at 335 nm (Figure 6B) is very similar to that observed for reduced *C. pasteurianum* rubredoxin⁵⁵ and is fit to a good approximation using the

Mössbauer-determined spin Hamiltonian parameters by varying the transition polarization. The best fit was obtained for a predominantly xy -polarized transition, i.e., M_{xy} , M_{xz} , M_{yz} in the ratio 1.0:0.2:0.2; see Figure 6B. Clearly both the Mössbauer and VTVH MCD saturation magnetization data indicate ground state properties for Fe(II) -bound NifIscA that are very similar to those of reduced rubredoxin. However, since the detailed ground state properties of Cys-to-Asp variants of reduced rubredoxin have yet to be determined, the observed ground state properties may also be consistent with a 4- or 5-coordinate Fe(II) sites involving three cysteinate and one or two oxygenic ligands as suggested by the anomalously low intensity and form of the VTMC spectra (see above).

Vibrational Properties. Resonance Raman was used to investigate Fe-S stretching modes in Fe(III) -bound NifIscA using visible excitation into CysS-to- Fe(III) charge transfer bands. The resonance Raman spectrum of Fe(III) -bound NifIscA in the Fe-S stretching region using 457.9-nm excitation is quite distinct compared to oxidized rubredoxins⁵⁸ and comprises a weak cysteine $\delta(\text{S-C-C})$ bending mode at $\sim 296 \text{ cm}^{-1}$ and symmetric and asymmetric Fe-S(Cys) stretching modes at 338 and 397 cm^{-1} , respectively; see Figure 7. Oxidized rubredoxins exhibit much greater resonance enhancement (at least 50-fold), with an intense symmetric breathing mode of the rhombically distorted tetrahedral Fe-(S(Cys))_4 unit between 312 and 318 cm^{-1} , three weak resolved asymmetric Fe-S(Cys) modes between 336 and 380 cm^{-1} , and internal bending modes of the coordinated cysteines at ~ 290 and $\sim 410 \text{ cm}^{-1}$.^{53,58} As shown in Figure 7, the resonance Raman spectrum of Fe(III) -bound NifIscA is much more similar to Cys-to-Asp rubredoxin variants that are coordinated by three cysteines and one monodentate or bidentate aspartate. For example, *C. pasteurianum* C6D rubredoxin exhibits a symmetric Fe-S(Cys) stretching mode at 335 cm^{-1} and an unresolved asymmetric Fe-S(Cys) stretching mode at 385 cm^{-1} , along with internal bending modes of the coordinated cysteines at 301 and 411 cm^{-1} .⁵³ Clearly the resonance Raman spectrum of Fe(III) -bound NifIscA can be interpreted in terms of a similar coordination environment to C6D rubredoxin, i.e., 4-coordinate with one noncysteine ligand or 5-coordinate with two noncysteine ligands or in terms symmetric and asymmetric Fe-S stretching involving two coordinated cysteine residues.

Redox Properties of Fe-Bound NifIscA . Since Fe(II) -bound NifIscA did not exhibit an X-band EPR spectrum in either parallel or perpendicular mode, monitoring the EPR intensity at $g = 5.5$ of samples frozen during dye-mediated redox titrations was used to determine the midpoint potential of the Fe(III)/Fe(II) couple. The results of reductive titration are shown in Figure 3B, and indicate a one-electron redox potential of $+36 \pm 15 \text{ mV}$ at pH 7.8 (versus NHE). Reversibility was demonstrated by restoration of $80 \pm 10\%$ of the initial intensity at $g = 5.5$ on oxidation to the initial starting potential. A similar level of reversibility ($\sim 75\%$) was observed using UV-visible absorption to monitor redox cycling using dithionite as the reductant and air as the oxidant, see Figure S2 in Supporting Information. Our inability to achieve full reversibility is likely to a consequence of greater lability for the Fe(II) -bound form. Although the cellular redox potential is primarily determined by two-electron dithiol/disulfide redox couples which are generally slow and inefficient in effecting one-electron redox processes, the high redox potential suggests that Fe-bound NifIscA will predominantly or exclusively be in the Fe(II) -bound state in a cellular environment under

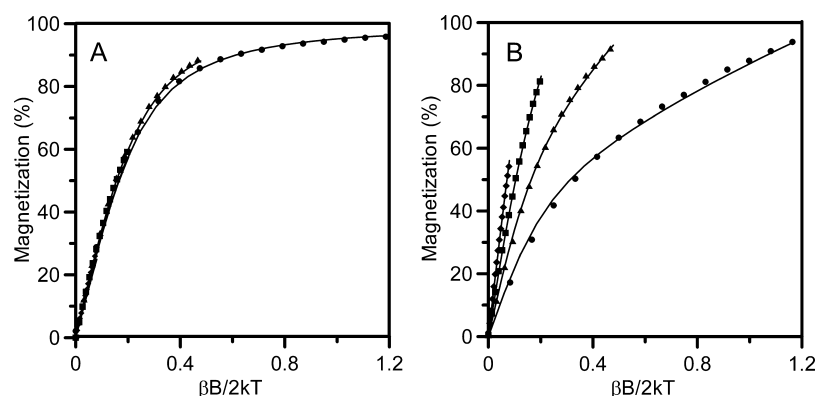


Figure 6. VHT MCD saturation magnetization data for Fe(III)- and Fe(II)-bound $NifIscA$. Samples are as described in Figure 2. (A) VHT MCD saturation magnetization data for Fe(III)-bound $NifIscA$ collected at 458 nm for magnetic fields between 0 and 6 T at temperatures of 1.73 K (●), 4.22 K (▲), 10.0 K (■), and 25.0 K (◆). Solid lines are theoretical fits for a predominantly xz -polarized electronic transition ($SM_{xy} = M_{xz} = SM_{yz}$) from a rhombic $S = 3/2$ ground state with zero-field splitting parameters $D = +3.0 \text{ cm}^{-1}$ and $E/D = 0.33$, and an isotropic real g -value of 2.0. (B) VHT MCD saturation magnetization data for Fe(II)-bound $NifIscA$ collected at 335 nm for magnetic fields between 0 and 6 T at temperatures of 1.73 K (●), 4.22 K (▲), 10.0 K (■), and 25.0 K (◆). Solid lines are theoretical fits for a predominantly xy -polarized electronic transition ($M_{xy} = SM_{xz} = SM_{yz}$) from an $S = 2$ ground state with zero-field splitting parameters $D = +7.6 \text{ cm}^{-1}$ and $E/D = 0.26$, and real g -values of $g_x = 2.11$, $g_y = 2.19$, and $g_z = 2.00$.

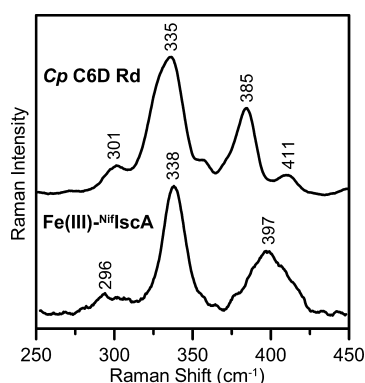


Figure 7. Comparison of the resonance Raman spectra of *C. pasteurianum* C6D rubredoxin (488-nm excitation) and Fe(III)-bound $NifIscA$ (458-nm excitation). Spectra were recorded at 17 K using samples that were 3–4 mM in protein monomer. Each spectrum is the sum of 100 scans, with each scan involving photon counting for 1 s every 0.5 cm^{-1} with a spectral bandwidth of 7 cm^{-1} . Raman bands originating from the frozen buffer solution have been subtracted from both spectra.

anaerobic growth conditions. However, the observation of Fe(III)-bound *A. vinelandii* $NifIscA$ in aerobic solutions containing THP or DTT (this work) and in Fe(III)-bound *E. coli* $IscA$ in aerobic solutions containing DTT and thioredoxin/thioredoxin,^{29,39} indicates that Fe(III)-bound of $NifIscA$ and $IscA$ is likely to be present in the cell under aerobic growth conditions. Hence both the Fe(III)- and Fe(II)-bound forms may be physiologically relevant with the oxidized form present primarily under aerobic growth conditions.

Cysteine-Mediated Release of Fe from Fe-Bound $NifIscA$. Previous studies by Ding and co-workers have demonstrated that the iron center in Fe(III)-bound *E. coli* $IscA$ is tightly bound with an association constant of $3.0 \times 10^{19} \text{ M}^{-1}$, but is specifically mobilized by cysteine when Fe(III)-bound $IscA$ is used as the Fe donor for Fe–S cluster assembly on $IscU$.³⁶ In accord with this result, addition of a 20-fold excess of L-cysteine to Fe(III)-bound $NifIscA$ under anaerobic conditions resulted in complete loss of the CysS-to-Fe(III) charge transfer bands associated with Fe(III)-bound $NifIscA$

within 20 min at 22 °C (data not shown). To address the possibility that cysteine is also competent to release Fe from Fe(II)-bound $NifIscA$, we utilized the ability of VT-MCD to selectively and quantitatively monitor Fe(II)-bound $NifIscA$; see Figure 8. The results indicate near complete release of Fe(II) from the Fe(II)-bound $NifIscA$ within 5 min of adding a 20-fold excess of L-cysteine, based on the close similarity of the resultant VT-MCD spectra compared to that obtained using the same concentration of ferrous ammonium sulfate in the presence of the same excess of L-cysteine under identical conditions. Moreover, analogous VT-MCD spectra were observed for the products of L-cysteine-mediated release of Fe from Fe(III)-bound measurements using Fe(III)-bound $NifIscA$ indicating that the Fe is released as Fe(II). We conclude that cysteine is competent to release Fe(II) from both the Fe(III)- and Fe(II)-bound forms of $NifIscA$.

$NifIscA$ as an Fe Donor for Cluster Assembly on $NifU$.

Previous studies of the time course of cysteine desulfurase-mediated $[2Fe-2S]^{2+}$ cluster assembly on U-type proteins using A-type proteins as Fe donors have been monitored by UV–visible absorption,^{29,35,37} which is of limited utility compared to UV–visible CD for distinguishing between $[2Fe-2S]^{2+}$ clusters in different protein environments or between $[2Fe-2S]^{2+}$ and $[4Fe-4S]^{2+}$ cluster formation. Moreover these studies have been carried out under conditions which favor rapid release of Fe^{2+} from Fe-bound A-type proteins (i.e., 37 °C and a 10–20 fold excess of L-cysteine) and hence are of limited use in assessing if A-type proteins function as Fe-donors by direct interprotein Fe transfer or cysteine-mediated release of free Fe^{2+} .

In this work, the ability of Fe-bound $NifIscA$ to function as an Fe donor for cluster assembly on $NifU$ was assessed by using UV–visible CD spectroscopy to compare the rates of $NifS$ -mediated $[2Fe-2S]$ cluster assembly on the N-terminal $IscU$ -like domain of $NifU$, termed $NifU-1$, using equivalent amounts of free Fe^{2+} ion and Fe-bound $NifIscA$ as the Fe source, under L-cysteine-limiting conditions at 22 °C; see Figure 9. Our previous spectroscopic studies of $NifS$ -mediated cluster assembly on full-length homodimeric $NifU$ and $NifU-1$ have demonstrated that cluster assembly is initiated by $[2Fe-2S]^{2+}$ cluster assembly on the N-terminal $IscU$ -like domain of each

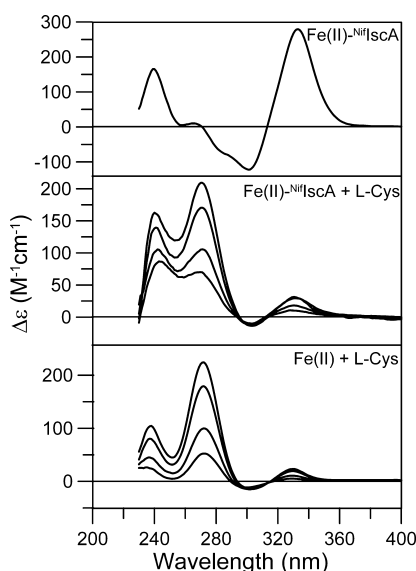


Figure 8. VTMCD evidence for Fe(II) release from Fe(II)-bound NifIscA in the presence of L-cysteine. All samples were in 100 mM Tris/HCl buffer, pH 7.8, with 55% v/v ethylene glycol, and were handled under anaerobic conditions. (Top) MCD spectra of Fe(II)- NifIscA recorded at 4.22 K with a magnetic field of 6 T. Sample was prepared by reducing a sample of Fe(III)-bound NifIscA (0.53 mM in NifIscA monomer with 0.5 Fe/monomer) with 0.3 mM sodium dithionite. (Middle) VTMCD spectra of the Fe(II)- NifIscA sample used in A after addition of a 20-fold excess of L-cysteine and incubating for 5 min prior to freezing for VTMCD studies. Spectra recorded at 4.22 K, 10.0 K, 25.0 K, and 50.0 K with a magnetic field of 6 T. (Bottom) VTMCD spectra of 0.12 mM ferrous ammonium sulfate in the presence of a 20-fold excess of L-cysteine and 0.2 mM sodium dithionite. Spectra recorded at 4.22 K, 10.0 K, 25.0 K, and 50.0 K with a magnetic field of 6 T. All MCD bands increase in intensity with decreasing temperature and $\Delta\epsilon$ values for all MCD spectra are based on Fe(II) concentration.

monomer, which leads to $[\text{4Fe-4S}]^{2+}$ cluster formation at the dimer interface and subsequent $[\text{4Fe-4S}]^{2+}$ cluster incorporation in the C-terminal domain.⁹ Hence NifU-1 was used for these studies to avoid interference from the permanent redox-active $[\text{2Fe-2S}]^{2+}$ cluster which exhibits intense CD spectra in both redox states (see accompanying paper). The time course of CD changes in a reaction mixture comprising 13 μM NifU-1, 108 μM Fe(III)-bound NifIscA (based on Fe concentration), 0.34 μM NifS, and 384 μM L-cysteine is shown in Figure 9A, with the red spectrum showing the CD spectrum of Fe(III)-bound NifIscA before the addition of L-cysteine to initiate the reaction. The marked differences in the UV-visible CD spectra of Fe(III)-bound NifIscA and the $[\text{2Fe-2S}]^{2+}$ cluster-bound forms of NifU-1 and NifIscA (Figure 9E) facilitate simultaneous monitoring of the release of Fe(II) from Fe(III)-bound NifIscA (Figure 9B) and the formation of $[\text{2Fe-2S}]^{2+}$ centers on both NifU-1 and NifIscA ; see Figure 9C. Notably, the CD spectra corresponding to $[\text{2Fe-2S}]^{2+}$ center formation change with time and can only be simulated assuming initial formation of $[\text{2Fe-2S}]^{2+}$ -NifU-1 and subsequent formation of $[\text{2Fe-2S}]^{2+}$ - NifIscA ; see Figure 9D.

Quantitation of each component as a function of time based on the $\Delta\epsilon$ values shown in Figure 9E, is shown in Figure 9F. The results show a pronounced lag in $[\text{2Fe-2S}]^{2+}$ cluster assembly on NifU-1 that correlates with a lag in cysteine-mediated release of Fe^{2+} from Fe(III)-bound NifIscA . Moreover, parallel experiments using identical conditions and the

equivalent concentration of free Fe^{2+} in place of Fe(III)-bound NifIscA show no lag phase and proceed at a rate comparable to that observed after the lag phase with Fe(III)-bound NifIscA as the Fe source. Taken together, these results indicate that the ability of Fe-bound NifIscA to function as an Fe donor for $[\text{2Fe-2S}]$ cluster assembly on NifU-1 requires L-cysteine-mediated release of free Fe(II), implying that it is a nonspecific Fe donor rather than a specific Fe donor that functions by direct interprotein Fe transfer.

Figure 9F also indicates that the generation of apo- NifIscA influences the final products of NifS-mediated cluster assembly on NifU-1 using Fe(III)-bound NifIscA as the Fe donor. In accord with previous Mössbauer studies of the time course of NifS-mediated cluster assembly on NifU-1 using a 9-fold excess of Fe^{2+} ,⁹ CD results under analogous conditions indicate the initial formation of the $[\text{2Fe-2S}]^{2+}$ cluster-bound form which maximizes at ~ 1 $[\text{2Fe-2S}]$ cluster/homodimer and subsequently decreases; see Figure 9F. Mössbauer studies have shown that the decrease results from the formation of $[\text{4Fe-4S}]^{2+}$ clusters, which exhibit negligible UV-visible CD intensity (see accompanying paper), via reductive coupling of $[\text{2Fe-2S}]^{2+}$ clusters assembled at the subunit interface of the homodimers.⁹ In contrast, when apo- NifIscA is generated by using Fe(III)-bound NifIscA as the Fe donor, the reaction yields fully loaded NifU-1 containing ~ 2 $[\text{2Fe-2S}]$ clusters/homodimer (corresponding to $\sim 32\%$ of the Fe released from Fe-bound NifIscA) and a major contribution of $[\text{2Fe-2S}]^{2+}$ cluster-bound NifIscA (corresponding to $\sim 45\%$ of the Fe released from Fe-bound NifIscA). There are two possibilities for the formation of $[\text{2Fe-2S}]^{2+}$ cluster-bound NifIscA . The first is that it occurs via NifS-mediated cluster assembly on apo- NifIscA ²⁴ once NifU-1 is almost replete with $[\text{2Fe-2S}]$ clusters. The second is that a $[\text{2Fe-2S}]$ cluster is directly transferred from NifU-1 to apo- NifIscA . At present it is not possible to assess if one or both of these processes are occurring. However, direct $[\text{2Fe-2S}]$ cluster transfer is supported by the observation that the second $[\text{2Fe-2S}]$ cluster assembled on the IscU homodimer has been shown to be much more labile than the first cluster,¹⁰ and that cluster incorporation on NifIscA only starts to occur when NifU-1 contains ~ 0.5 clusters/homodimer; see Figure 9F. Furthermore, evidence for cluster transfer from NifU to NifIscA is presented in the accompanying paper. Hence it is possible that NifIscA is functioning as both a nonspecific Fe donor for $[\text{2Fe-2S}]$ cluster assembly on NifU-1 and an acceptor of $[\text{2Fe-2S}]$ clusters generated on NifU-1 in this in vitro reaction.

DISCUSSION

The iron binding studies of *A. vinelandii* NifIscA presented in this work complement and extend the studies carried out by Ding and co-workers with *E. coli* IscA and SufA and human ISCA1. However, prior to this work, there was no evidence for a high-affinity Fe(III)-bound form of NifIscA . By using THP rather than DTT to cleave disulfides or polysulfides on NifIscA , we were able to demonstrate high affinity Fe(III) binding and to obtain homogeneous samples of Fe(III)-bound NifIscA containing one intermediate spin ($S = 3/2$) Fe(III) center per NifIscA dimer in accord with the published results obtained for *E. coli* IscA and SufA and human ISCA1.^{29,32,35} Moreover, the excited state electronic properties and the ground state electronic and vibrational properties of this novel intermediate-spin Fe(III) center have been characterized in detail using UV-visible absorption, CD and VTMCD, EPR, Mössbauer

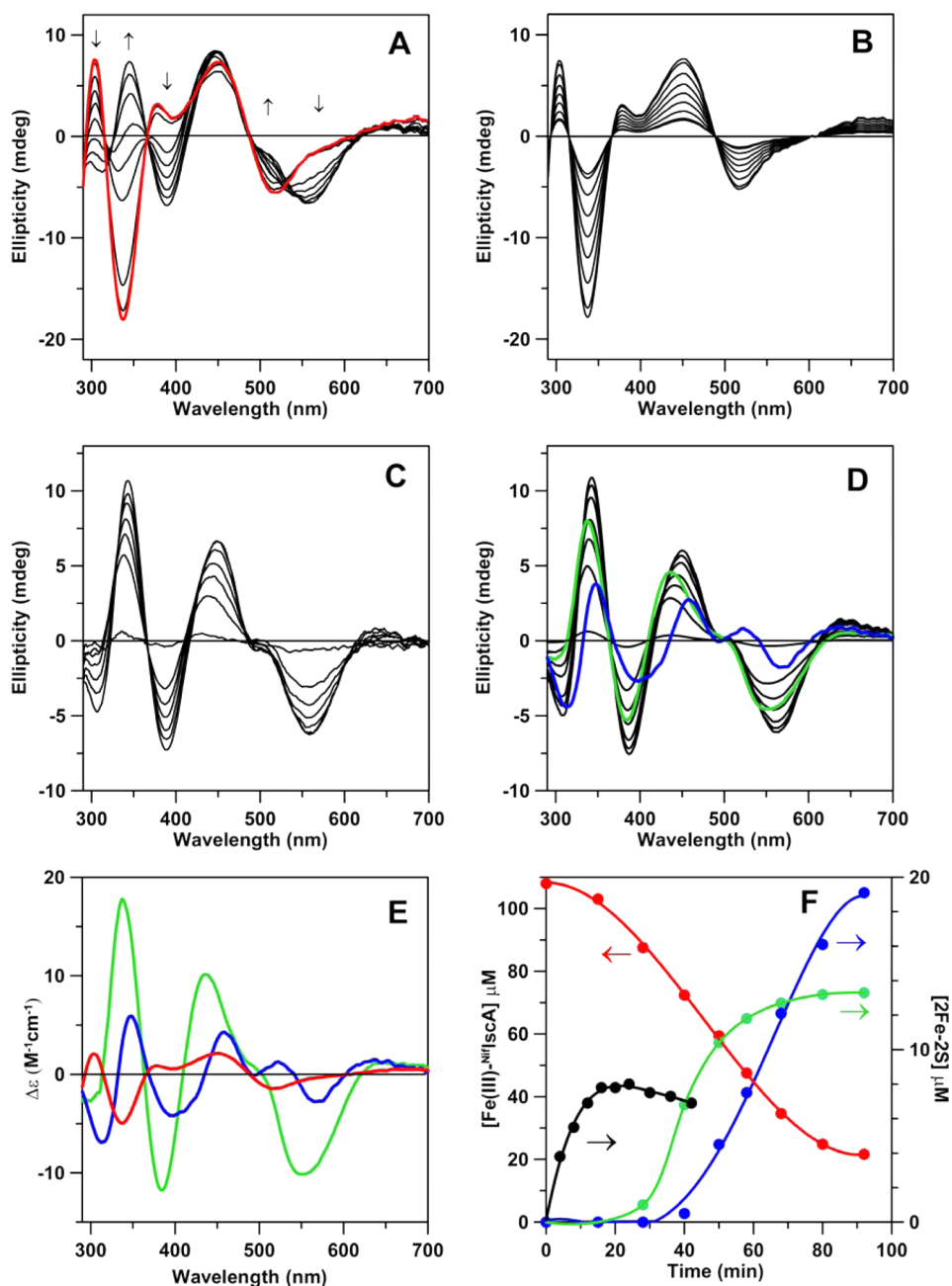


Figure 9. CD studies of [2Fe-2S] cluster assembly on NifU-1 using Fe(III)-bound NifIscA as the iron donor. (A) CD time course of a reaction mixture (volume 600 μM in 1 cm cuvette) comprising 13 μM NifU-1, 108 μM Fe(III)-bound NifIscA (based on Fe concentration), 0.34 μM NifS, and 384 μM L-cysteine in 100 mM Tris-HCl buffer, pH 7.5, at 22 °C. Spectra were recorded at 0, 15, 28, 40, 50, 58, 68, 80, and 92 min after initiating the reaction by the addition of L-cysteine. The red spectrum corresponds to the zero-time spectrum, i.e., 108 μM Fe(III)-bound NifIscA in the same volume of reaction mixture without NifU-1, NifS, and L-cysteine. The arrows indicate the direction of change in CD intensity with increasing time at discrete wavelengths. Spectra at each time point were resolved into decreasing contributions from the Fe(III)-bound NifIscA component (B) and an increasing combined contribution from the [2Fe-2S] cluster-bound forms of NifU-1 and NifIscA (C). The 0 and 15 min spectra in C have negligible CD intensity and have been omitted for clarity. (D) Simulation of the CD spectra in C based on contributions from the CD spectra of [2Fe-2S] cluster-bound forms of NifU-1 and NifIscA . The individual contributions from the [2Fe-2S] cluster-bound forms of NifU-1 and NifIscA that were used to simulate the 92 min spectrum in C are shown as green and blue lines, respectively. (E) CD spectra for Fe(III)-bound NifIscA (red), [2Fe-2S] cluster-bound NifU-1 (green), and [2Fe-2S] cluster-bound NifIscA (blue) with $\Delta\epsilon$ values based on Fe or [2Fe-2S] cluster concentration. (F) Computed changes in the concentrations of Fe(III)-bound NifIscA (red), [2Fe-2S] cluster-bound NifU-1 (green), and [2Fe-2S] cluster-bound NifIscA (blue) in the reaction mixture, based on the CD $\Delta\epsilon$ values shown in E. The black data points and line correspond to the concentration of [2Fe-2S] cluster-bound NifU-1 as a function of time in a control CD experiment using the same reaction mixture with 108 μM ferrous ammonium sulfate in place of 108 μM Fe(III)-bound NifIscA .

and resonance Raman spectroscopies. The results indicate the first example of a rhombic ($E/D = 0.33$) intermediate-spin ($S = 3/2$) Fe(III) center with thiolate ligation. Pure intermediate-

spin Fe(III) complexes are uncommon and the majority are axial 5-coordinate square pyramidal complexes with porphyrin, dithiocarbamate, or macrocyclic tetraamido ligands.⁵⁹ Since the

overwhelming majority of intermediate spin Fe(III) complexes are five coordinate and the resonance Raman and UV–visible absorption and VTMC results for Fe(III)-bound $\text{Nif}^{\text{H}}\text{IscA}$ are best interpreted in terms of two or three cysteinate ligands, this suggests the presence of two or three noncysteine ligands.

This work also demonstrates one-electron redox cycling between Fe(III)/(II)-bound forms of $\text{Nif}^{\text{H}}\text{IscA}$ with a redox potential of $+36 \pm 15$ mV at pH 7.8 (vs NHE). A well-defined Fe(II)-bound form of other A-type proteins has not been reported. This is probably a consequence of lower binding affinity for Fe(II) compared to Fe(III) and the fact that the Fe(II)-bound form is more difficult to detect than the Fe(III)-bound form since it does not exhibit an X-band EPR signal and is only evident in the UV–visible absorption spectrum by a band at 320 nm, the same wavelength as the most intense absorption of the Fe(III)-bound form and of bound polysulfides. Nevertheless the Fe(II)-bound form is stable in solution under anaerobic conditions and readily detected and characterized using VTMC and Mössbauer spectroscopies. The results indicate a rhombic high-spin ($S = 2$) Fe(II) species with properties similar to reduced rubredoxins or rubredoxin variants with three cysteinate and one or two oxygenic ligands. Although the one-electron redox potential for the Fe(III)/(II)-bound forms of $\text{Nif}^{\text{H}}\text{IscA}$ indicates that Fe(II)-bound form is likely to be the dominant Fe-bound form in cells under anaerobic growth conditions, the observation of the Fe(III)-bound forms of $\text{Nif}^{\text{H}}\text{IscA}$ and IscA in aerobic dithiol/disulfide buffering media indicates that the oxidized form is likely to be present in the cell under aerobic growth conditions. Moreover, the observation that L-cysteine mediates Fe(II) release from both the Fe(III) and Fe(II)-bound forms of $\text{Nif}^{\text{H}}\text{IscA}$ indicates that both forms have the potential to function as Fe donors to U-type scaffold proteins with the former functioning under aerobic growth conditions and the later functioning under anaerobic growth conditions. This observation also argues against the possibility that the Fe-bound forms, particularly the Fe(II)-bound form, constitute the initial precursors for *de novo* cysteine desulfurase-mediated cluster biosynthesis on A-type proteins, since the cysteine substrate which supplies the S for cluster assembly would also promote release of bound Fe.

The inability of other research groups to observe high affinity Fe(III) binding in three archetypical A-type proteins, *A. vinelandii* $\text{Nif}^{\text{H}}\text{IscA}$ ²⁴ and *E. coli* IscA and SufA ^{40,60} had previously raised doubts concerning the biological significance of the Fe-bound A-type proteins reported by Ding and co-workers. For *A. vinelandii* $\text{Nif}^{\text{H}}\text{IscA}$, the current work demonstrates that the initial failure to observe high-affinity Fe(III) binding was a consequence of the inability of DTT to reduce disulfide or polysulfides involving the Fe-binding cysteine residues. In addition, the close similarity in the absorption and EPR properties of the novel mononuclear $S = 3/2$ Fe(III) center in *A. vinelandii* $\text{Nif}^{\text{H}}\text{IscA}$ compared to those previously reported for mononuclear $S = 3/2$ Fe(III) centers in *E. coli* IscA and SufA and human ISCA1 ,^{29,32,35} leaves little doubt that high affinity Fe(III) binding is a common property of A-type proteins.

The question that therefore needs to be addressed is whether or not Fe-bound A-type proteins are present in vivo. A definitive answer is currently not available, since, to our knowledge, this question has yet to be addressed for any organism under normal growth conditions. Moreover, it is unclear if physiologically relevant levels of Fe-bound A-type proteins can exist in the presence of normal cellular levels of L-cysteine, which have been estimated to be in the 0.1–0.2 mM

range in *E. coli*.⁶¹ However, in vivo characterization of recombinant proteins in *S. cerevisiae* has provided convincing evidence for a Fe-bound rather than Fe–S cluster-bound form of a IscA1/IscA2/Iba57 complex.³⁰ Iba57 is a tetrahydrofolate-dependent protein with bacterial homologues (YgfZ in *E. coli*) that appears to play a key role in facilitating Fe release from the IscA1/IscA2 to appropriate acceptor proteins.³⁰ Hence it is possible that Iba57 and its bacterial homologue protect against indiscriminant cysteine-dependent Fe release for A-type proteins in both yeast and bacteria.

In contrast the situation is far from clear when the in vivo status is inferred from the composition of recombinant overexpressed bacterial A-type proteins as purified. The majority, including *A. vinelandii* investigated herein and *E. coli* IscA and SufA ,^{25,26} are purified under aerobic conditions as apo proteins. This is surprising if they function as Fe storage or donor proteins in vivo in view of the high binding affinity for Fe(III). While the origin of this discrepancy has yet to be fully resolved, it may be a consequence of lack of coexpression of the Iba57 homologue or aerobic overexpression of recombinant proteins that are unable to bind Fe due to oxidative dithiol or polysulfide formation involving the active site cysteines, as demonstrated for $\text{Nif}^{\text{H}}\text{IscA}$ in this work. In contrast, Ding and co-workers have purified Fe(III)-bound forms of recombinant human ISCA1 and *E. coli* IscA/SufA under aerobic conditions^{29,32,35} and shown that Fe incorporation increases when the aerobic growth medium was supplemented with ferrous ammonium sulfate³⁵ and ferric citrate,⁴² respectively. These results demonstrate the potential for recombinant, overexpressed A-type proteins to store Fe(III) in an accessible form for Fe–S cluster assembly under aerobic growth conditions.

It is also important to note that a few recombinant A-type proteins contain Fe–S clusters as purified, i.e., the structurally characterized *T. elongatus* IscA ²³ and *E. coli* SufA (when coexpressed with SufBCDSE)¹⁶ which both contain $[2\text{Fe-2S}]$ clusters and *Acidithiobacillus ferrooxidans* IscA which contains a $[4\text{Fe-4S}]$ cluster.⁶² Indeed, the observation that *E. coli* SufA is purified as a $[2\text{Fe-2S}]$ -containing protein when coexpressed with the other components of the *suf* operon provides compelling evidence for the physiological relevance of cluster-bound forms of A-type proteins. As discussed below and in the accompanying paper, the ability of A-type proteins to bind Fe–S clusters is best rationalized in terms of a role as cluster carriers for delivering clusters assembled on the U-type and SufB -type scaffold proteins to acceptor proteins. Since the results presented herein argue strongly against the possibility that Fe(III)-bound A-type proteins are the products of aerial oxidation of cluster-bound forms during purification, the available data are consistent with the possibility that both Fe- and cluster-bound A-type proteins are functional forms that are present in vivo.

The above discussion demonstrates that there is a growing body of in vitro and in vivo evidence suggesting a physiological role for Fe-bound forms of bacterial and eukaryotic A-type proteins. Hence the next question that needs to be addressed is whether or not Fe-bound A-type proteins serve as Fe donors for cluster assembly on U-type scaffold proteins as proposed by the work of Ding and co-workers. The results presented herein using Fe-bound $\text{Nif}^{\text{H}}\text{IscA}$, coupled with the previously published studies using human ISCA1 and *E. coli* IscA and SufA ,^{29,32,35} clearly demonstrate that A-type proteins are competent Fe donors for in vitro cysteine desulfurase-mediate cluster assembly on the appropriate U-type scaffold proteins. However,

CD-monitored cluster assembly on NifU-1 using Fe(III)-bound Nif⁺IsaC is shown here to occur by L-cysteine-mediated release of free Fe(II) rather than by direct interprotein Fe transfer. This suggests that Fe-bound A-type proteins are not specific Fe donors for U-type proteins, but have the potential to contribute to a pool of free Fe(II) that may be available for cluster assembly on scaffold proteins. While this is possible, it should be stressed that there is currently no *in vivo* evidence in support of a role for A-type proteins as Fe donors to primary scaffold proteins. In *A. vinelandii*, no growth phenotype has been reported for Nif⁺iscA knockouts and a null-growth phenotype has only been observed for depletion of IscA for growth under elevated O₂.³¹ However, the lack of a phenotype for individual Av⁺Nif⁺IsaC and IscA knockouts under normal aerobic growth conditions may be a consequence of functional redundancy, as has been shown to the case of IscA and SufA in *E. coli*.^{27,32} In yeast, where there is *in vivo* evidence for an Fe-bound form of Isa1/Isa2, ⁵⁵Fe-immunoprecipitation studies indicated that depletion of Isa1 and Isa2 results in a slight increase in Fe associated with Isu1, indicating that the Fe-bound Isa1/Isa2 complex cannot be the sole Fe donor for cluster assembly on Isu1.³⁰

The only other candidate for the immediate Fe donor to U-type scaffold proteins is frataxin (yeast Yfh1) and the bacterial homologue CyaY. Physical interactions and structural studies have implicated involvement of the frataxin in the yeast Nfs1/Isd11/IscU1 and bacterial IscS/IscU Fe–S cluster assembly complexes^{63,64} and recent *in vitro* studies implicate a role as an allosteric regulator of these biosynthetic complexes.^{65,66} Moreover, Yfh1 deficiency does result in defective Fe–S cluster biosynthesis on Isu1,⁶⁷ which is consistent with a role as an Fe donor. However, neither Yfh1 nor CyaY are essential for viability in yeast and *E. coli*, respectively,⁶⁸ and the Fe binding affinity is weak (micromolar range) and associated with surface carboxylates,^{69,70} which argues against a role in cellular Fe trafficking. Nevertheless, it is possible that frataxin and CyaY function as immediate Fe donors for cluster assembly on Isu1 and IscU, respectively, by functioning as Fe(II)-dependent allosteric regulators that trigger sulfur delivery and channel Fe to the assembly site in the complex.

The recent *in vivo* evidence that A-type proteins are specifically required for the maturation of [4Fe-4S] proteins but are not required for the maturation of [2Fe-2S] proteins, is also difficult to reconcile with a role as a primary Fe-donor to U-type proteins which are required for the maturation of both [2Fe-2S] and [4Fe-4S] proteins. The *iscA* and *sufA* double knockouts in *E. coli* have demonstrated an essential and specific role for A-type proteins in the maturation of [4Fe-4S] centers under aerobic growth conditions,^{27,32,33} and *S. cerevisiae* Isa1/Isa2 and human ISCA1/ISCA2 have been shown to be specifically required for effective maturation of mitochondrial [4Fe-4S] proteins.^{30,34} In bacteria this *in vivo* function of A-type proteins has been interpreted in terms of roles as specific cluster carriers for the delivery of clusters assembled on U-type or SufB-type primary scaffold proteins. The cluster carrier hypothesis is supported by *in vitro* studies which indicate that IscA can accept Fe–S clusters from IscU²⁶ and that SufA can accept Fe–S clusters from the SufBCD complex,⁷¹ and by recent phylogenomic and genetic studies of the interdependence of the three A-type proteins in *E. coli*, i.e., IscA, SufA, and ErpA.^{4,27} A cluster carrier role for Nif⁺IsaC is also demonstrated in the accompanying paper which provides *in vitro* evidence that Nif⁺IsaC has the ability to function as an oxygen-tolerant

Fe–S cluster carrier protein for the delivery of clusters assembled on NifU in nitrogen fixation-specific Fe–S cluster biogenesis.

An alternative role for Fe-bound A-type proteins that is implicated by the recent *in vivo* studies of *S. cerevisiae* Isa1 and Isa2³⁰ is that they function downstream of U-type or SufB-type primary scaffold proteins as specific Fe donors for the maturation of [4Fe-4S] clusters on acceptor proteins. *In vitro* studies have demonstrated assembly of [4Fe-4S]²⁺ clusters on bacterial U-type proteins via reductive coupling of two [2Fe-2S]²⁺ at the subunit interface proteins^{9,13} and intact transfer of these [4Fe-4S] clusters to acceptor proteins.^{8,9,11} However, the assembly and transfer of U-type [4Fe-4S] clusters in bacteria are only viable under strictly anaerobic conditions due to the acute oxygen sensitivity of the [4Fe-4S] center. Consequently an alternative mechanism is required in the presence of oxygen and the *in vivo* knockout data clearly implicate a role for A-type proteins in the maturation or repair of [4Fe-4S] clusters under aerobic growth conditions.^{27,33} Since U-type proteins are required under both aerobic and anaerobic growth conditions and do not require A-type proteins for the assembly of the more oxygen-tolerant [2Fe-2S] centers, it seems likely that they are initial source of the [2Fe-2S] units for [4Fe-4S] cluster assembly under both aerobic and anaerobic conditions. Hence under aerobic conditions it is possible that bacterial [4Fe-4S] clusters are assembled on acceptor proteins *in situ* using [2Fe-2S] clusters initially formed on U-type proteins and Fe provided by A-type proteins. On the basis of the available data, an analogous [4Fe-4S] cluster assembly pathway appears to have been adopted under both aerobic and anaerobic growth conditions in yeast.³⁰ This begs the question as to the source of the additional S.

One possibility that has emerged from our recent studies of the Fumarate Nitrate Reduction (FNR) regulatory protein is that the additional S is present in the form of partial cysteine persulfide ligation of the bound [2Fe-2S] cluster.⁷² Resonance Raman and mass spectrometry studies of FNR have demonstrated that O₂-induced degradation of the [4Fe-4S]²⁺ cluster results in a [2Fe-2S]²⁺ cluster with two cysteine persulfide ligands that can be reconverted back to initial [4Fe-4S]²⁺ cluster under anaerobic conditions by addition of Fe(II) in the presence of a dithiol reagent. Moreover, resonance Raman has provided evidence that analogous cysteine persulfide-ligated [2Fe-2S]²⁺ clusters are formed by O₂-induced degradation of [4Fe-4S]²⁺ centers in radical-SAM enzymes. Hence Fe-bound A-type proteins could be specific Fe donors for cysteine persulfide-ligated [2Fe-2S]²⁺ clusters, formed by IscU-generated [2Fe-2S]²⁺ cluster binding to cysteine desulfurase-generated cysteine persulfides or by O₂-induced degradation [4Fe-4S]²⁺ clusters, for the *in situ* repair or maturation of [4Fe-4S] centers on acceptor proteins. As discussed in the accompanying paper, the IscU-generated [2Fe-2S]²⁺ clusters are likely to be delivered to acceptor proteins by [2Fe-2S]²⁺ cluster-bound A-type proteins. In addition, Fe-bound A-type proteins may function in the repair of cubane-type [3Fe-4S]⁺ that are initially generated by O₂-exposure of the site-differentiated [4Fe-4S]²⁺ centers in radical-SAM, (de)hydratases and IspG/IspH enzymes.^{73–76} In dithiol/disulfide buffering media these clusters can be reduced to the [3Fe-4S]⁰ forms which avidly incorporates Fe(II) to generate the original [4Fe-4S]²⁺ cluster.⁷⁴ These proposed roles for Fe-bound A-type proteins in the assembly and repair of biological [4Fe-4S] clusters are summarized schematically in Figure 10.

of the hypothetical protein AQ-1857 encoded by the Y157 gene from *Aquifex aeolicus* reveals a novel protein fold. *Proteins: Struct. Funct. Bioinform.* 54, 794–796.

(23) Morimoto, K., Yamashita, E., Kondou, Y., Lee, S. J., Arisaka, F., Tsukihara, T., and Nakai, M. (2006) The asymmetric IscA homodimer with an exposed [2Fe-2S] cluster suggests the structural basis of the Fe-S cluster biosynthetic scaffold. *J. Mol. Biol.* 360, 117–132.

(24) Krebs, C., Agar, J. N., Smith, A. D., Frazzon, J., Dean, D. R., Huynh, B. H., and Johnson, M. K. (2001) IscA, an alternative scaffold for Fe-S cluster biosynthesis. *Biochemistry* 40, 14069–14080.

(25) Ollagnier-de-Choudens, S., Mattioli, T., Takahashi, Y., and Fontecave, M. (2001) Iron-sulfur cluster assembly. Characterization of IscA and evidence for a specific functional complex with ferredoxin. *J. Biol. Chem.* 276, 22604–22607.

(26) Ollagnier-de-Choudens, S., Sanakis, Y., and Fontecave, M. (2004) SufA/IscA: reactivity studies of a class of scaffold proteins involved with [Fe-S] cluster assembly. *J. Biol. Inorg. Chem.* 9, 828–838.

(27) Vinella, D., Brochier-Armanet, C., Loiseau, L., Talla, E., and Barras, F. (2009) Iron-sulfur (Fe/S) protein biogenesis: Phylogenomic and genetic studies of A-type carriers. *PLoS Genet.* 5, e1000497.

(28) Balasubramanian, R., Shen, G., Bryant, D. A., and Golbeck, J. H. (2006) Regulatory roles for IscA and SufA in iron homeostasis and redox stress responses in the cyanobacterium *Synechococcus* sp. strain PCC 7002. *J. Bacteriol.* 188, 3182–3191.

(29) Ding, H., and Clark, R. J. (2004) Characterization of iron-binding in IscA, an ancient iron-sulfur cluster assembly protein. *Biochem. J.* 379, 433–440.

(30) Mühlenhoff, U., Richter, N., Pines, O., Pierik, A. J., and Lill, R. (2011) Specialized function of yeast Isa1 and Isa2 in the maturation of mitochondrial [4Fe-4S] proteins. *J. Biol. Chem.* 286, 41205–41216.

(31) Johnson, D. C., Unciuleac, M.-C., and Dean, D. R. (2006) Controlled expression and functional analysis of iron-sulfur cluster biosynthetic components within *Azotobacter vinelandii*. *J. Bacteriol.* 188, 7551–7561.

(32) Lu, J., Yang, J., Tan, G., and Ding, H. (2008) Complementary roles of SufA and IscA in the biogenesis of iron-sulfur clusters in *Escherichia coli*. *Biochem. J.* 409, 535–543.

(33) Tan, G., Lu, J., Bitoun, J. P., Huang, H., and Ding, H. (2009) IscA/SufA paralogues are required for the [4Fe-4S] cluster assembly in enzymes of multiple physiological pathways in *Escherichia coli* under aerobic growth conditions. *Biochem. J.* 420, 463–472.

(34) Sheftel, A. D., Wilbrecht, C., Stehling, O., Niggemeyer, B., Elsässer, H.-P., Mühlenhoff, U., and Lill, R. (2012) The human mitochondrial ISCA1, ISCA2, and IBA57 proteins are required for [4Fe-4S] protein maturation. *Mol. Biol. Cell* 23, 1157–1166.

(35) Lu, J., Bitoun, J. P., Tan, G., Wang, W., Min, W., and Ding, H. (2010) Iron-binding activity of human iron-sulfur cluster assembly protein hIscA1. *Biochem. J.* 428, 125–131.

(36) Ding, B., Smith, E. S., and Ding, H. (2005) Mobilization of the iron centre in IscA for the iron-sulfur cluster assembly in IscU. *Biochem. J.* 389, 797–802.

(37) Ding, H., Clark, R. J., and Ding, B. (2004) IscA mediates iron delivery for assembly of iron-sulfur clusters in IscU under limited “free” iron conditions. *J. Biol. Chem.* 279, 37499–37504.

(38) Bitoun, J. P., Wu, G., and Ding, H. (2008) *Escherichia coli* FtnA acts as an iron buffer for re-assembly of iron-sulfur clusters in response to hydrogen peroxide. *BioMetals* 21, 693–703.

(39) Ding, H., Harrison, K., and Lu, J. (2005) Thioredoxin reductase system mediates iron binding in IscA and iron-delivery for the iron-sulfur cluster assembly in IscU. *J. Biol. Chem.* 280, 30432–30437.

(40) Yang, J., Bitoun, J. P., and Ding, H. (2006) Interplay of IscA and IscU in biogenesis of iron-sulfur clusters. *J. Biol. Chem.* 281, 27956–27963.

(41) Ding, H., Yang, J., Coleman, L. C., and Yeung, S. (2007) Distinct iron binding property of two putative iron donors for the iron-sulfur cluster assembly: IscA and the bacterial frataxin ortholog CyaY under physiological and oxidative stress conditions. *J. Biol. Chem.* 282, 7997–8004.

(42) Wang, W., Huang, H., Tan, G., Fan, S., Liu, M., Landry, A. P., and Ding, H. (2010) *In vivo* evidence for the iron-binding activity of an iron-sulfur cluster assembly protein IscA in *Escherichia coli*. *Biochem. J.* 432, 429–436.

(43) Sendra, M., Ollagnier de Choudens, S., Lascoux, D., Sanakis, Y., and Fontecave, M. (2007) The SUF iron-sulfur cluster biosynthetic machinery: Sulfur transfer from the SUFS-SUFE complex to SUFA. *FEBS Lett.* 581, 1362–1368.

(44) Yuvaniyama, P., Agar, J. N., Cash, V. L., Johnson, M. K., and Dean, D. R. (2000) NifS-directed assembly of a transient [2Fe-2S] cluster within the NifU protein. *Proc. Natl. Acad. Sci. U.S.A.* 97, 599–604.

(45) Agar, J. N., Yuvaniyama, P., Jack, R. F., Cash, V. L., Smith, A. D., Dean, D. R., and Johnson, M. K. (2000) Modular organization and identification of a mononuclear iron-binding site within the NifU protein. *J. Biol. Inorg. Chem.* 5, 167–177.

(46) Brown, R. E., Jarvis, K. L., and Hyland, K. J. (1989) Protein measurement using bicinchoninic acid: elimination of interfering substances. *Anal. Biochem.* 180, 136–139.

(47) Fish, W. W. (1988) Rapid colorimetric micromethod for the quantitation of complexed iron in biological samples. *Methods Enzymol.* 158, 357–364.

(48) Drozdowski, P. M., and Johnson, M. K. (1988) A simple anaerobic cell for low temperature Raman spectroscopy. *Appl. Spectrosc.* 42, 1575–1577.

(49) Johnson, M. K. (1988) in *Metal Clusters in Proteins* (Que, L., Jr., Ed.) pp 326–342, American Chemical Society, Washington, DC.

(50) Thomson, A. J., Cheesman, M. R., and George, S. J. (1993) Variable-temperature magnetic circular dichroism. *Methods Enzymol.* 226, 199–232.

(51) Neese, F., and Solomon, E. I. (1999) MCD C-term signs, saturation behavior, and determination of band polarizations in randomly oriented systems with spin $S \geq 1/2$. Applications to $S = 1/2$ and $S = 5/2$. *Inorg. Chem.* 38, 1847–1865.

(52) Ravi, N., Bollinger, J. M., Huynh, B. H., Edmondson, D. E., and Stubbe, J. (1994) Mechanism of assembly of the tyrosyl radical-diiron(III) cofactor of *E. coli* ribonucleotide reductase. 1. Mössbauer characterization of the diferric radical precursor. *J. Am. Chem. Soc.* 116, 8007–8014.

(53) Staples, C. R. (1997) Structure-Function Relationships in Iron-Sulfur Proteins, Ph.D. Thesis, University of Georgia.

(54) Kennepohl, P., Neese, F., Schweitzer, D., Jackson, H. L., Kovacs, J. A., and Solomon, E. I. (2005) Spectroscopy of a non-heme iron thiolate complexes: Insight into the electronic structure of the low-spin active site of nitrile hydratase. *Inorg. Chem.* 44, 1826–1836.

(55) Werth, M. T., and Johnson, M. K. (1989) Magnetic circular dichroism and electron paramagnetic resonance studies of Fe(II)-metallothionein. *Biochemistry* 28, 3982–3988.

(56) Schulz, C., and Debrunner, P. G. (1976) Rubredoxin, a simple iron-sulfur protein: Its spin Hamiltonian and hyperfine parameters. *J. Phys. Colloques* 37, C6–153–158.

(57) Vrajmasu, V. V., Bominaar, E. L., Meyer, J., and Münck, E. (2002) Mössbauer study of reduced rubredoxin as purified and in whole cells. Structural correlation analysis of spin Hamiltonian parameters. *Inorg. Chem.* 41, 6358–6371.

(58) Czernuszewicz, R. S., LeGall, J., Moura, I., and Spiro, T. G. (1986) Resonance Raman spectra of rubredoxin: new assignments and vibrational coupling mechanism from iron-54/iron-56 isotope shifts and variable-wavelength excitation. *Inorg. Chem.* 25, 696–700.

(59) Kostka, K. L., Fox, B. G., Hendrich, M. P., Collins, T. J., Rickard, C. E. F., Wright, L. J., and Munck, E. (1993) High-valent transition metal chemistry. Mössbauer and EPR studies of high-spin ($S = 2$) iron(IV) and intermediate-spin ($S = 3/2$) iron(III) complexes with a macrocyclic tetraamido-N ligand. *J. Am. Chem. Soc.* 115, 6746–6757.

(60) Fontecave, M., and Ollagnier-de-Choudens, S. (2008) Iron-sulfur cluster biosynthesis in bacteria: Mechanisms of cluster assembly and transfer. *Arch. Biochem. Biophys.* 474, 226–237.

- (61) Park, S., and Imlay, J. A. (2003) High levels of intracellular cysteine promote oxidative DNA damage by driving Fenton reaction. *J. Bacteriol.* 185, 1942–1950.
- (62) Zeng, J., Geng, M., Jiang, H., Liu, Y., Liu, J., and Qiu, G. (2007) The IscA from *Acidithiobacillus ferrooxidans* is an iron-sulfur protein which assemble the $[\text{Fe}_4\text{S}_4]$ cluster with intracellular iron and sulfur. *Arch. Biochem. Biophys.* 463, 237–244.
- (63) Gerber, J., Mühlenhoff, U., and Lill, R. (2003) An interaction between frataxin and Isu1/Nfs1 that is crucial for Fe/S cluster synthesis on Isu1. *EMBO Rep.* 4, 907–911.
- (64) Shi, R., Proteau, A., Villarroja, M., Moukadiri, I., Zhang, L., Trempe, J.-F., Matte, A., Armengod, M. E., and Cygler, M. (2010) Structural basis for Fe-S cluster assembly and tRNA thiolation mediated by IscS protein-protein interactions. *PLoS Biol.* 8, e1000354.
- (65) Adinolfi, S., Iannuzzi, C., Prisch, F., Pastore, C., Iametti, S., Martin, S. R., Bonomi, F., and Pastore, A. (2009) Bacterial frataxin CyaY is the gatekeeper of iron-sulfur cluster formation catalyzed by IscS. *Nat. Struct. Mol. Biol.* 16, 390–396.
- (66) Tsai, C.-L., and Barondeau, D. P. (2010) Human frataxin is an allosteric switch that activates the Fe-S cluster biosynthetic complex. *Biochemistry* 49, 9132–9139.
- (67) Mühlenhoff, U., Gerber, J., Richhardt, N., and Lill, R. (2003) Components involved in assembly and dislocation of iron-sulfur clusters on the scaffold protein IscUlp. *EMBO J.* 22, 4815–4825.
- (68) Li, D. S., Ohshima, K., Jiralspong, S., Bojanowski, M. W., and Pandolfo, M. (1999) Knock-out of the cyaY gene in *Escherichia coli* does not affect cellular iron content and sensitivity to oxidants. *FEBS Lett.* 456, 13–16.
- (69) Cook, J. D., Bencze, K. Z., Jankovic, A. D., Crater, A. K., Busch, C. N., Bradley, P. B., Stemmler, A. J., Spaller, M. R., and Stemmler, T. L. (2006) Monomeric yeast frataxin is an iron binding protein. *Biochemistry* 45, 7767–7777.
- (70) Stemmler, T. L., Lesuisse, E., Pain, D., and Dancis, A. (2010) Frataxin and mitochondrial FeS cluster biogenesis. *J. Biol. Chem.* 285, 26737–26743.
- (71) Chahal, H. K., Dai, Y., Saini, A., Ayala-Castro, C., and Outten, F. W. (2009) The SufBCD Fe-S scaffold complex interacts with SufA for Fe-S cluster transfer. *Biochemistry* 48, 10644–10653.
- (72) Zhang, B., Crack, J. C., Subramanian, S., Green, J., Thomson, A. J., Le Brun, N. E., and Johnson, M. K. (2012) Reversible cycling between cysteine persulfide-ligated $[2\text{Fe-2S}]$ and cysteine-ligated $[4\text{Fe-4S}]$ clusters in the FNR regulatory protein. *Proc. Natl. Acad. Sci. U.S.A.* 109, 15734–15739.
- (73) Beinert, H., Kennedy, M. C., and Stout, C. D. (1996) Aconitase as iron-sulfur protein, enzyme, and iron-regulatory protein. *Chem. Rev.* 96, 2335–2373.
- (74) Johnson, M. K., Duderstadt, R. E., and Duin, E. C. (1999) Biological and synthetic $[\text{Fe}_3\text{S}_4]$ clusters. *Adv. Inorg. Chem.* 47, 1–82.
- (75) Johnson, M. K., Smith, A. D. (2005) in *Encyclopedia of Inorganic Chemistry*, 2nd ed., (King, R. B., Ed.) pp 2589–2619, John Wiley & Sons, Chichester.
- (76) Grawert, T., Kaiser, J., Zepeck, F., Laupitz, R., Hecht, S., Amslinger, N., Schramek, N., Schlicher, E., Weber, S., Haslbeck, M., Buchner, J., Rieder, C., Arigoni, D., Bacher, A., and Eisenreich, W. (2004) IspH protein of *Escherichia coli*: Studies on iron-sulfur cluster implementation and catalysis. *J. Am. Chem. Soc.* 126, 12847–12855.